THE ASTROPHYSICAL JOURNAL, 402:479–492, 1993 January 10


# OBSCURATION OF QUASARS BY DUST IN DAMPED LYMAN-ALPHA SYSTEMS

S. MICHAEL FALL
Space Telescope Science Institute, 3700 San Martin Drive, Baltimore, MD 21218
AND
YICHUAN C. PEI
Princeton University Observatory, Peyton Hall, Princeton, NJ 08544
*Received 1991 December 2; accepted 1992 July 16*

## ABSTRACT

We present a largely analytical method to compute the obscuration of quasars by dust in damped Ly$\alpha$ absorption systems. The inputs required by our method are the observed luminosity function of quasars and the typical dust-to-gas ratio and empirical distribution of H I column densities in the damped Ly$\alpha$ systems. We use the dust-to-gas ratio inferred from the reddening of background quasars in our previous studies. As outputs, we obtain self-consistent corrections for the effects of obscuration on the luminosity function of quasars and the distribution of H I column densities in the damped Ly$\alpha$ systems. Our calculations indicate that 10%–70% of the bright quasars at $z = 3$ are missing from optical samples. This is not enough obscuration to explain the flattening or turnover in the observed comoving density of bright quasars in the interval $2 \lesssim z \lesssim 3$. It does, however, help to account for the ultraviolet background radiation implied by the proximity effect at $z \approx 3$. We estimate that quasars produce at least 10% and possibly all of this radiation. According to our extrapolations, the obscuration increases so rapidly with redshift that samples of optically selected quasars may be only 10% complete at $z = 4$. The uncertainties in our estimates of the obscuration are caused mainly by the weak constraints on the number of damped Ly$\alpha$ systems with the highest H I column densities. For the same reason, we can only set weak constraints on the comoving densities of H I and dust in the damped Ly$\alpha$ systems: $1 \times 10^{-3} \lesssim h\Omega_{\rm H\,I} \lesssim 3 \times 10^{-2}$ and $10^{-6} \lesssim h\Omega_{\rm dust} \lesssim 10^{-4}$. The limits from *COBE* on the far-infrared background radiation imply that the dust in the damped Ly$\alpha$ systems cannot be much hotter than the dust in the Milky Way.

*Subject headings:* dust, extinction — quasars: absorption lines

## 1. INTRODUCTION

This paper is a continuation of our study of the reddening and obscuration of quasars by dust in damped Ly$\alpha$ absorption systems (Fall & Pei 1989, hereafter Paper I; Fall, Pei, & McMahon 1989, hereafter Paper II; Pei, Fall, & Bechtold 1991, hereafter Paper III). We are motivated by two important suggestions: (1) that obscuration by dust in galactic disks could seriously bias the observed counts of optically selected quasars at high redshifts (Ostriker & Heisler 1984) and (2) that the damped Ly$\alpha$ systems are the high-redshift analogs or progenitors of present-day galactic disks (Wolfe et al. 1986). The obscuration, if severe, could distort our picture of the evolution of quasars and their contribution to the background radiation at ultraviolet and other wavelengths. There have been several attempts to quantify such effects but often with conflicting results (Ostriker & Heisler 1984; Wright 1986; Boissé & Bergeron 1988; Heisler & Ostriker 1988; Najita, Silk, & Wachter 1990; Ostriker, Vogeley, & York 1990; Wright 1990). While some of these studies used limited information about the damped Ly$\alpha$ systems, most of them involved different assumptions about the number density and linear sizes of the intervening galaxies and the abundance, internal distribution, and extinction curve of the dust. Our approach has been to rely as heavily as possible on the observed properties of the damped Ly$\alpha$ systems.

We have previously estimated the abundance of dust in the damped Ly$\alpha$ systems from the reddening of background quasars. This involves a comparison of the spectral indices of quasars with and without damped Ly$\alpha$ systems along the lines of sight. Our results are expressed in terms of the dimensionless dust-to-gas ratio $k \equiv 10^{21}(\tau_B/N_{\rm H\,I})$ cm$^{-2}$, where $\tau_B$ is the extinction optical depth in the rest-frame $B$ band, and $N_{\rm H\,I}$ is the column density of neutral atomic hydrogen. We ignore molecular hydrogen because it is much less abundant than H I in the damped Ly$\alpha$ systems (Chaffee, Black, & Foltz 1988; Lanzetta, Wolfe, & Turnshek 1989, and references therein). For a given reddening, $k$ depends on the slope of the extinction curve at ultraviolet wavelengths (1200–2200 Å). We use the mean extinction curves in the Milky Way and the Large and Small Magellanic Clouds (GAL, LMC, and SMC). Paper I describes our method in detail, while Papers II and III report the detection and confirmation of dust in two independent samples. The most probable values of the dust-to-gas ratio in the damped Ly$\alpha$ systems, derived from the observed reddening with the three different extinction curves, are $k_p = 0.35^{+0.24}_{-0.09}$ (GAL), $k_p = 0.09^{+0.06}_{-0.02}$ (LMC), and $k_p = 0.06^{+0.03}_{-0.01}$ (SMC). Galactic-type dust is probably ruled out by the absence of strong extinction features near 2175 Å in the rest frames of the damped Ly$\alpha$ systems, whereas LMC-type dust is marginally acceptable from this point of view, and SMC-type dust is completely acceptable. Our best estimates of the typical dust-to-gas ratio in the damped Ly$\alpha$ systems are therefore 5%–20% of the value $k \approx 0.8$ in the Milky Way. These are consistent with recent estimates based on the depletion of Cr relative to Zn in several damped Ly$\alpha$ systems (Meyer, Welty, & York 1989; Meyer & Roth 1990; Pettini, Boksenberg, & Hunstead 1990; see Paper III for a critical discussion).

In this paper, we combine the typical dust-to-gas ratio from

Paper III with the empirical distribution of H I column densities from Lanzetta et al. (1991) to estimate the obscuration of quasars by dust in damped Ly$\alpha$ systems. Specifically, we compute the mean optical depth along random lines of sight and the ratio of the true and observed luminosity functions of quasars. This would be straightforward but for two complications. First, since the distribution of H I column densities was determined from damped Ly$\alpha$ systems in the foreground of optically selected quasars, it is potentially biased by the very obscuration we wish to estimate. We derive the formulae necessary to correct this bias in § 2 and estimate the true distribution of H I column densities in § 3. Second, the obscuration depends on damped Ly$\alpha$ systems at all redshifts, while the dust-to-gas ratio and the distribution of H I column densities are known only in a limited range of redshifts ($2 \lesssim z \lesssim 3$). In § 4, we extrapolate to higher and lower redshifts and then estimate the true comoving density of bright quasars and their contribution to the ultraviolet background radiation. Our results are summarized and discussed in § 5. Many of the calculations presented in the main text of this paper are based on the simplifying assumption that all damped Ly$\alpha$ systems at a given redshift have the same dust-to-gas ratio. We show in the Appendix that even a relatively large dispersion in the dust-to-gas ratio would have little effect on our main conclusions.

## 2. MATHEMATICAL FORMULATION

We derive in this section some basic relations between the obscuration of quasars and the distribution of H I column densities in the damped Ly$\alpha$ systems. We begin by defining $p_t(\tau \mid z)d\tau$ as the probability that the total optical depth in a random direction to a redshift $z$ lies between $\tau$ and $\tau + d\tau$. The subscript $t$ is used here to distinguish "true" quantities from those biased by obscuration (see below). All optical depths in this section pertain to a fixed wavelength at $z = 0$, which we take to be the effective wavelength of the $B$ band, with $\lambda_B = 4400$ Å. The probability density $p_t$ contains all statistical information about the obscuration, and any other measure can be computed from it. One of the simplest is the mean optical depth, given by

$$\bar{\tau}_t(z) = \int_0^\infty d\tau \tau p_t(\tau \mid z) . \quad (1)$$

If dust were distributed uniformly in space, the optical depth would be the same in all directions, and we would have $p_t(\tau \mid z) = \delta[\tau - \bar{\tau}_t(z)]$, where $\delta$ denotes the Dirac delta function. However, for discrete absorbers, such as the damped Ly$\alpha$ systems, there may be large variations in the optical depth in different directions. In this case, $\bar{\tau}_t$ provides only a partial, and potentially misleading, account of the obscuration. We include it here mainly for comparison with previous work.

The other measure of obscuration we consider is the ratio of the true and observed luminosity functions of quasars. By definition, $\phi_t(L, z)dL$ is the true number of quasars per unit comoving volume at a redshift $z$ with absolute luminosities between $L$ and $L + dL$, and $\phi_o(L, z)dL$ is the corresponding "observed" number. We showed in Paper I that $\phi_t$ and $\phi_o$ are related by

$$\phi_o(L, z) = \int_0^\infty d\tau e^\tau \phi_t(e^\tau L, z) p_t(\tau \mid z) . \quad (2)$$

For consistency with the optical depths, the luminosities in this expression must be determined from apparent magnitudes in the $B$ band. Given $p_t$ and $\phi_o$, equation (2) can be inverted by the method in Paper I to obtain $\phi_t$. The ratio $\phi_t/\phi_o$ can then be interpreted as a "correction factor" for the effects of obscuration. In this paper, we consider only the obscuration by dust in damped Ly$\alpha$ systems. Other biases that could affect the observed luminosity function of quasars include obscuration by intergalactic dust and magnification by gravitational lenses. The former would increase $\phi_t/\phi_o$ with respect to our estimates, while the latter would decrease $\phi_t/\phi_o$ (at high luminosities). We defer a quantitative assessment of these effects to subsequent papers.

We now turn to the problem of determining the true probability density $p_t$ from the observed properties of the damped Ly$\alpha$ systems. This is complicated by the fact that the absorbers are discovered in the spectra of optically selected quasars and, as a result of obscuration, may be underrepresented in such samples. We must therefore distinguish between random lines of sight, which can point in any direction, and observed lines of sight, which point only toward optically selected quasars. With this in mind, we define $p_o(\tau \mid z)d\tau$ as the probability that the total optical depth along an observed line of sight to a redshift $z$ lies between $\tau$ and $\tau + d\tau$. For a magnitude-limited sample, $p_o(\tau \mid z)$ must be proportional to $p_t(\tau \mid z)$ and the fraction of quasars at the redshift $z$ that are bright enough to be included in the sample when obscured by an optical depth $\tau$:

$$p_o(\tau \mid z) \propto p_t(\tau \mid z) \int_{e^\tau L_l(z)}^\infty dL \phi_t(L, z) \Big/ \int_{L_l(z)}^\infty dL \phi_t(L, z) . \quad (3)$$

Here, $L_l(z)$ is the absolute luminosity of a quasar at a redshift $z$ that would just appear at the limiting magnitude of the sample if there were no obscuration. The coefficient of proportionality in equation (3) must ensure that $p_o(\tau \mid z)$ is normalized with respect to $\tau$ for all $z$. This condition, together with equation (2), implies

$$p_o(\tau \mid z) \int_{L_l(z)}^\infty dL \phi_o(L, z) = p_t(\tau \mid z) \int_{e^\tau L_l(z)}^\infty dL \phi_t(L, z) . \quad (4)$$

Equations (3) and (4) should be applicable to the Lanzetta et al. (1991) sample, which is approximately magnitude limited at $B_l \approx 19$.

The probability densities $p_t$ and $p_o$ describe the cumulative effects of obscuration by all absorbers along random and observed lines of sight. For some purposes, however, it is desirable to relate these quantities to the statistics of individual absorbers. Thus, we define $\rho_t(\tau, z)d\tau\, dz$ and $\rho_o(\tau, z)d\tau\, dz$, respectively, as the mean numbers of absorbers along random and observed lines of sight with optical depths between $\tau$ and $\tau + d\tau$ and redshifts between $z$ and $z + dz$. The functions $\rho_t$ and $\rho_o$ are related to $p_t$ and $p_o$ by

$$\frac{\partial p_t(\tau \mid z)}{\partial z} = \int_0^\tau d\tau' p_t(\tau - \tau' \mid z) \rho_t(\tau', z) - p_t(\tau \mid z) \int_0^\infty d\tau' \rho_t(\tau', z) , \quad (5)$$

$$\frac{\partial p_o(\tau \mid z)}{\partial z} = \int_0^\tau d\tau' p_o(\tau - \tau' \mid z) \rho_o(\tau', z) - p_o(\tau \mid z) \int_0^\infty d\tau' \rho_o(\tau', z) , \quad (6)$$

with the boundary conditions $p_t(\tau \mid 0) = p_o(\tau \mid 0) = \delta(\tau)$. Equation (5) was derived in Paper I, and equation (6) follows from the same kind of reasoning. The Fourier transform of equation (5) is equivalent to the formulae presented by Wright (1986).

The only assumption here is that the redshifts of the absorbers are not correlated on the scales of interest. This is certainly true for the damped Ly$\alpha$ systems, which have typical separations $\Delta z \sim 3$ along the line of sight. Using equations (1) and (5), the mean optical depth can be reexpressed in the form

$$\bar{\tau}_t(z) = \int_0^z dz' \int_0^\infty d\tau \tau \rho_t(\tau, z') . \quad (7)$$

To make further progress, we must adopt a specific model for the observed luminosity function of quasars. The standard representation of $\phi_o(L, z)$, at least for $z \lesssim 2.2$, is a double power law in $L$ (Boyle, Shanks, & Peterson 1988). However, since we are mainly interested in bright quasars at high redshifts, a single power law should suffice:

$$\phi_o(L, z) = \psi_o(z) L^{-\beta-1} \quad \text{for} \quad L > 4 \times 10^{12}\, L_\odot . \quad (8)$$

The lower limit on $L$, corresponding to $M_B = -26$, is dictated by some comparisons made in § 4 and by the faintest quasars in the Lanzetta et al. (1991) sample. We determine the exponent $\beta$ in equation (8) from the luminosity function presented by Hartwick & Schade (1990). This includes more than $10^3$ optically selected quasars with magnitudes measured in the $B$ band from 15 independent surveys. Most of the quasars with $z \lesssim 2.2$ were discovered by the UVX method, while most of those with $z \gtrsim 2.2$ were discovered by multicolor and spectroscopic methods. Hartwick & Schade tabulate the luminosity function for a Hubble constant of 50 km s$^{-1}$ Mpc$^{-1}$ and two extreme combinations of the deceleration parameter $q_0$ and the spectral index $\alpha$ used in the $K$-corrections. Figure 1 shows the results for $(q_0, \alpha) = (0.1, -1.0)$ in four intervals of redshift covering the range $1.7 \leq z \leq 3.3$. Evidently, a single power law provides an acceptable fit over the specified range in luminosity. Weighted, least-square solutions give $\beta = 1.7 \pm 0.1$ for $(q_0, \alpha) = (0.1, -1.0)$ and $\beta = 2.3 \pm 0.2$ for $(q_0, \alpha) = (0.5, -0.5)$. As a compromise, we adopt $\beta = 2.0$ in all the calculations reported here.

The power-law model simplifies enormously the relation between the true and observed luminosity functions of quasars. Equations (2) and (8) imply $\phi_t(L, z) = \psi_t(z) L^{-\beta-1}$, with

$$\psi_o(z)/\psi_t(z) = \int_0^\infty d\tau p_t(\tau \mid z) \exp(-\beta\tau) . \quad (9)$$

Multiplying equation (4) by $\exp(+\beta\tau)$ and integrating with respect to $\tau$ gives the alternative relation

$$\psi_t(z)/\psi_o(z) = \int_0^\infty d\tau p_o(\tau \mid z) \exp(+\beta\tau) . \quad (10)$$

The right-hand sides of equations (9) and (10) can be reexpressed in terms of $\rho_t$ and $\rho_o$ using equations (5) and (6):

$$\psi_o(z)/\psi_t(z) = \exp\left\{\int_0^z dz' \int_0^\infty d\tau \rho_t(\tau, z')[\exp(-\beta\tau) - 1]\right\} , \quad (11)$$

$$\psi_t(z)/\psi_o(z) = \exp\left\{\int_0^z dz' \int_0^\infty d\tau \rho_o(\tau, z')[\exp(+\beta\tau) - 1]\right\} . \quad (12)$$

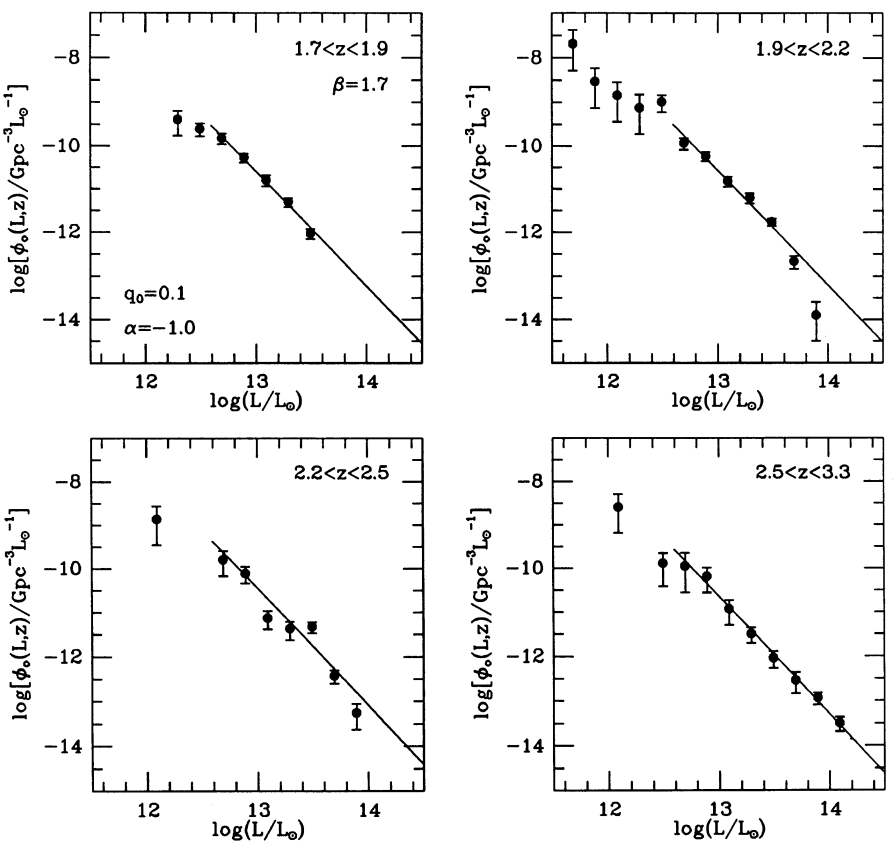


FIG. 1.—Observed luminosity function of quasars from Hartwick & Schade (1990) for $h = 0.5$ and $(q_0, \alpha) = (0.1, -1.0)$. The lines are weighted, least-square fits in the form of eq. (8) with $\beta = 1.7$.

Multiplying equation (11) by equation (12) and differentiating with respect to $z$ gives

$$\int_0^\infty d\tau[\exp(-\beta\tau) - 1][\rho_t(\tau, z) - \rho_o(\tau, z)\exp(+\beta\tau)] = 0 . \quad (13)$$

Since this must hold for arbitrary $\rho_t$ or $\rho_o$, we have the simple result

$$\rho_t(\tau, z)/\rho_o(\tau, z) = \exp(+\beta\tau) . \quad (14)$$

To simplify the remaining analysis, we now assume that the dust-to-gas ratio $k$ is the same in all damped Ly$\alpha$ systems at a given redshift. We refer to this as a "constant" dust-to-gas ratio, even though it may vary with redshift. In this case, $\rho_t$ and $\rho_o$ are uniquely related to the true and observed distributions of H I column densities. Following Tytler (1987), we define $f_t(N, z)dN\,dX$ and $f_o(N, z)dN\,dX$, respectively, as the mean numbers of absorbers along random and observed lines of sight with H I column densities between $N$ and $N + dN$ and "absorption distances" between $X$ and $X + dX$. In a Friedmann universe, with vanishing cosmological constant, increments of absorption distance and redshift are related by $dX = (1 + z)(1 + 2q_0 z)^{-1/2} dz$ (Bahcall & Peebles 1969). Thus, we have

$$\rho_t(\tau, z)d\tau = (1 + z)(1 + 2q_0 z)^{-1/2} f_t(N, z)dN , \quad (15)$$

$$\rho_o(\tau, z)d\tau = (1 + z)(1 + 2q_0 z)^{-1/2} f_o(N, z)dN . \quad (16)$$

Furthermore, the optical depth in the rest frame of an observer at $z = 0$ is related to the H I column density of an absorber by

$$\tau = \left(\frac{kN}{10^{21}\ \mathrm{cm}^{-2}}\right)\xi\left(\frac{\lambda_B}{1 + z}\right) , \quad (17)$$

where $\xi(\lambda)$ is the ratio of the extinction at a wavelength $\lambda$ to that in the $B$ band.

We can now express all quantities of interest in terms of the distribution of H I column densities in the damped Ly$\alpha$ systems. Substituting equations (15) and (17) into equation (7) gives

$$\bar{\tau}_t(z) = 104h\int_0^z dz' \frac{k(z')\Omega_{\mathrm{H\,I}}(z')(1 + z')}{(1 + 2q_0 z')^{1/2}}\,\xi\left(\frac{\lambda_B}{1 + z'}\right) , \quad (18)$$

where $h$ is the Hubble constant in units of 100 km s$^{-1}$ Mpc$^{-1}$, and

$$\Omega_{\mathrm{H\,I}}(z) = \frac{8\pi G m_{\mathrm{H}}}{3cH_0}\int_0^\infty dN N f_t(N, z) \quad (19)$$

is the mean comoving density of H I in units of the present critical density. From equations (11) or (12), and (14)–(17), we have

$$\frac{\psi_t(z)}{\psi_o(z)} = \exp\left\{\int_0^z dz' \frac{(1 + z')}{(1 + 2q_0 z')^{1/2}}\int_0^\infty dN[f_t(N, z') - f_o(N, z')]\right\} , \quad (20)$$

$$\frac{f_t(N, z)}{f_o(N, z)} = \exp\left[\beta\left(\frac{kN}{10^{21}\ \mathrm{cm}^{-2}}\right)\xi\left(\frac{\lambda_B}{1 + z}\right)\right] . \quad (21)$$

These are the desired relations between missing quasars and missing damped Ly$\alpha$ systems in the case of a constant dust-to-gas ratio. In the Appendix, we generalize equations (18), (20), and (21) to the case of a variable dust-to-gas ratio.

## 3. DISTRIBUTION OF H I COLUMN DENSITIES

In principle, we could use the formulae derived in the previous section to compute all quantities of interest directly from the empirical (i.e., discrete) distribution of H I column densities in a sample of damped Ly$\alpha$ systems. However, unless the sample were huge, the results would be dominated by a few absorbers with the highest H I column densities. To reduce this sensitivity, we adopt a plausible model for the true distribution $f_t$, compute the corresponding observed distribution $f_o$ from equation (21), and adjust the parameters in the model to obtain acceptable fits to the empirical distribution. We assume for simplicity that the damped Ly$\alpha$ systems are planar disks with radial H I profiles $N_\perp(r)$ when viewed face-on. In our analysis, it proves convenient to invert the profiles (assumed to be monotonic functions) and write $r = g(N_\perp/N_{\perp 0})$, where $N_{\perp 0}$ is the central H I column density. When a disk is viewed at an angle $\theta = \cos^{-1}\mu$ to the normal, a circle of radius $r$ projects to an ellipse with an area $A = \pi\mu r^2$. Expressing this in terms of the H I column density along the line of sight, $N = N_\perp/\mu$, we have

$$A(N, \mu) = \pi\mu g^2(\mu N/N_{\perp 0}) \quad \text{for} \quad 0 \le \mu \le \mu_m \equiv \min\{1, N_{\perp 0}/N\} , \quad (22)$$

where the upper limit on $\mu$ follows from the conditions $\theta \ge 0$ and $r \ge 0$. The true distribution of H I column densities, allowing for random orientations of the disks, is then

$$f_t(N, z) = \frac{cn_D}{H_0}\int_0^{\mu_m} d\mu\left|\frac{\partial A(N, \mu)}{\partial N}\right| = \frac{\pi c n_D}{H_0 N_{\perp 0}}\left(\frac{N_{\perp 0}}{N}\right)^3\int_0^{\mu_m N/N_{\perp 0}} dx x^2\left|\frac{dg^2(x)}{dx}\right| , \quad (23)$$

where $n_D$ is the mean number of disks per unit comoving volume.

We now assume that the radial H I profiles in the damped Ly$\alpha$ systems have exponential form: $N_\perp(r) = N_{\perp 0}\exp(-\alpha r)$. The H I profiles in spiral galaxies at the present epoch show a wide variety of forms, but the sum of the H I and $H_2$ profiles can often be approximated by exponential functions with scale lengths similar to those of the stellar disks (Young & Scoville 1991). Since the damped Ly$\alpha$ systems at $2 \lesssim z \lesssim 3$ have very little $H_2$, most of the neutral gas must be in the form of H I, and it is at least plausible that the profiles are roughly exponential. This model also facilitates comparisons between our results and those of Heisler & Ostriker (1988) and Wright (1990). Fortunately, none of our conclusions depends critically on the adopted form of the H I profiles. The inverse of the exponential profile is $g(x) = -\alpha^{-1}\ln x$. Substituting this into equation (23), we obtain

$$f_t(N, z) = \frac{\pi c n_D \mu_m^2}{2H_0\alpha^2 N}\left[1 - 2\ln\left(\frac{\mu_m N}{N_{\perp 0}}\right)\right] , \quad (24)$$

with $\mu_m = 1$ for $N \le N_{\perp 0}$ and $\mu_m = N_{\perp 0}/N$ for $N \ge N_{\perp 0}$. In the limit $N \ll N_{\perp 0}$, we have $f_t(N, z) \propto N^{-1}\ln N$, and in the opposite limit, $N \gg N_{\perp 0}$, we have $f_t(N, z) \propto N^{-3}$.

It is worth pausing here to consider the parameters that enter $f_t$ and thus $f_o$. These are: the mean number of disks per unit comoving volume $n_D$, the central H I column density $N_{\perp 0}$,

and the exponential scale length $\alpha^{-1}$. We prefer to eliminate $n_D$ and $\alpha^{-1}$ in favor of the mean comoving density of neutral hydrogen $\Omega_{\rm H\,I}$ as follows. Inserting $f_t$ from equation (24) into equation (19) gives

$$\Omega_{\rm H\,I} = \frac{16\pi^2 G m_{\rm H} n_D N_{\perp 0}}{3H_0^2 \alpha^2} . \quad (25)$$

This is equivalent to $\Omega_{\rm H\,I} = 8\pi G n_D M_{\rm H\,I}/3H_0^2$, where $M_{\rm H\,I} = 2\pi m_{\rm H} N_{\perp 0}/\alpha^2$ is the H I mass of an exponential disk. We now have, from equations (24) and (25),

$$f_t(N, z) = 2.6 \times 10^{22} \frac{h\Omega_{\rm H\,I}\mu_m^2}{NN_{\perp 0}}\left[1 - 2\ln\left(\frac{\mu_m N}{N_{\perp 0}}\right)\right] \text{cm}^{-2} . \quad (26)$$

In this form, the true distribution depends only on the parameters $h\Omega_{\rm H\,I}$ and $N_{\perp 0}$. The elimination of $n_D$ and $\alpha^{-1}$ is important because there are very few observational constraints on the number density and linear sizes of the damped Ly$\alpha$ systems. Moreover, since $\alpha^{-1}$ no longer appears in $f_t$, equation (26) is equally valid for a population of absorbers with a wide range of scale lengths.

Figure 2 shows the empirical distribution of H I column densities in the damped Ly$\alpha$ system from Lanzetta et al. (1991). This is based on 30 confirmed and eight candidate damped Ly$\alpha$ lines with $N \geq 2 \times 10^{20}$ cm$^{-2}$ in the spectra of 156 quasars, including those in the samples of Wolfe et al. (1986) and Sargent, Steidel, & Boksenberg (1989). Most of the damped Ly$\alpha$ systems have redshifts in the range $2 \lesssim z \lesssim 3$. Also shown in Figure 2 are the distributions of H I column densities in Lyman-limit systems ($10^{17} \lesssim N \lesssim 10^{20}$ cm$^{-2}$) and Ly$\alpha$ forest systems ($N \lesssim 10^{17}$ cm$^{-2}$) from Tytler (1987) and Sargent et al. (1989). The dashed lines are the power-law approximations derived by these authors. As noted by Lanzetta et al., the distribution of H I column densities in the damped Ly$\alpha$ systems is significantly higher than the extrapolated power laws. Integrating over the empirical distributions, we find that the damped Ly$\alpha$ systems contain at least 10 times as much neutral hydrogen as the Lyman-limit and Ly$\alpha$ forest systems combined. This is a lower limit because $\Omega_{\rm H\,I}$ depends mainly on systems with the highest H I column densities, where the empirical distribution lacks a well-defined cutoff. In the following, we ignore the Lyman-limit and Ly$\alpha$ forest systems; the former may be associated with galactic halos, while the latter are probably intergalactic clouds.

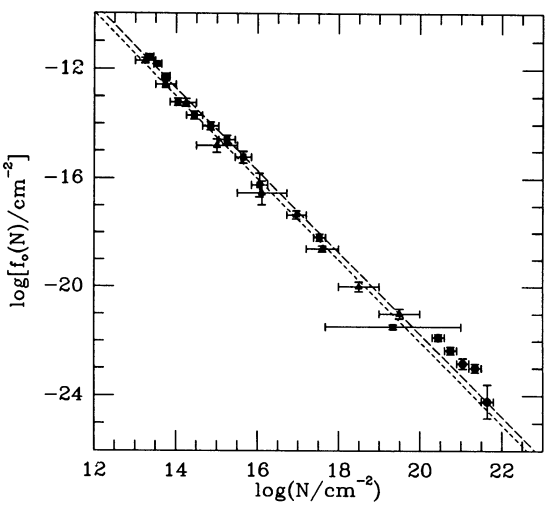


FIG. 2.—Empirical distributions of H I column densities in quasar absorption-line systems for $q_0 = 0$. The circles are for damped Ly$\alpha$ systems with $1.7 \leq z \leq 3.4$ (Lanzetta et al. 1991), the triangles are for Lyman-limit systems with $0.4 \leq z \leq 3.3$ and Ly$\alpha$ forest systems with $1.9 \lesssim z \lesssim 2.1$ (Tytler 1987), and the squares are for Lyman-limit systems with $2.5 \leq z \leq 3.6$ and Ly$\alpha$ forest systems with $3.4 \lesssim z \lesssim 3.8$ (Sargent et al. 1989). The short-dashed line is from Tytler, and the long-dashed line is from Sargent et al.

We compare the model distribution $f_o$ for randomly oriented exponential disks with the empirical distribution for damped Ly$\alpha$ systems using the likelihood-ratio test. The advantage of this test is that it does not require binning of the H I column densities or redshifts. To simplify the analysis, we assume that the parameters $h\Omega_{\rm H\,I}$ and $N_{\perp 0}$ are independent of redshift (over the range $2 \lesssim z \lesssim 3$). The likelihood function relevant to our problem is then

$$L(h\Omega_{\rm H\,I}, N_{\perp 0}) = \prod_a [(1 + z_a)(1 + 2q_0 z_a)^{-1/2} f_o(N_a, z_a)\delta N\, \delta z] \times \exp\left[-\sum_e \int_{z_{\rm min}^e}^{z_{\rm max}^e} dz \frac{(1+z)}{(1+2q_0 z)^{1/2}} \int_{N_{\rm min}}^{\infty} dN f_o(N, z)\right], \quad (27)$$

with $f_o$ given by equations (21) and (26). Here, $N_a$ and $z_a$ are the H I column density and redshift of the $a$th absorber (from Turnshek et al. 1989 and Lanzetta et al. 1991), $z_{\rm min}^e$ and $z_{\rm max}^e$ are the minimum and maximum redshifts at which damped Ly$\alpha$ lines could have been detected in the spectrum of the $e$th quasar (from Wolfe et al. 1986 and Lanzetta et al. 1991), and $N_{\rm min} = 2 \times 10^{20}$ cm$^{-2}$ is the H I column density above which the detections are reasonably complete. The product is over all confirmed and candidate damped Ly$\alpha$ systems with $N \geq N_{\rm min}$, and the sum is over all quasars in the Lanzetta et al. sample. Equation (27), based on Poisson statistics, gives the probability of finding exactly one damped Ly$\alpha$ system in each of the small intervals $\delta N$ and $\delta z$ centered on $N_a$ and $z_a$ and none in any of the other accessible intervals of $N$ and $z$. The best-fit parameters maximize $L(h\Omega_{\rm H\,I}, N_{\perp 0})$, and confidence contours derive from the fact that $-2\ln[L(h\Omega_{\rm H\,I}, N_{\perp 0})/L_{\rm max}]$ is distributed as $\chi^2$ with two degrees of freedom.

We have computed the likelihood function without dust and with LMC-type dust for three values of the dust-to-gas ratio: $k = 0.05$, 0.10, and 0.20. The dust-free case is included for comparison, while $0.05 \leq k \leq 0.20$ is essentially the 2 $\sigma$ confidence interval derived from the observed reddening with the LMC extinction curve (Paper III). Figure 3 shows the 1, 2, and 3 $\sigma$ confidence contours for the parameters $h\Omega_{\rm H\,I}$ and $N_{\perp 0}$ (solid curves) and the maxima of $L(h\Omega_{\rm H\,I}, N_{\perp 0})$ with respect to $N_{\perp 0}$ at constant $h\Omega_{\rm H\,I}$ (dashed curves). The cross in the upper left-hand panel indicates the best-fit parameters without dust. In this case, our estimate of $h\Omega_{\rm H\,I}$ is only about 30% higher than the one obtained by Lanzetta et al. (1991) from a direct sum over the damped Ly$\alpha$ systems. However, when we include dust, the confidence contours become so elongated, indicating such strong correlations between $h\Omega_{\rm H\,I}$ and $N_{\perp 0}$, that the best-fit parameters are no longer meaningful. The orientation of the contours is such that $h\Omega_{\rm H\,I}/N_{\perp 0}$, and hence the fraction of the sky covered by the absorbers, is nearly constant. That the two parameters cannot be determined separately is a consequence of the relatively featureless form of the empirical distribution

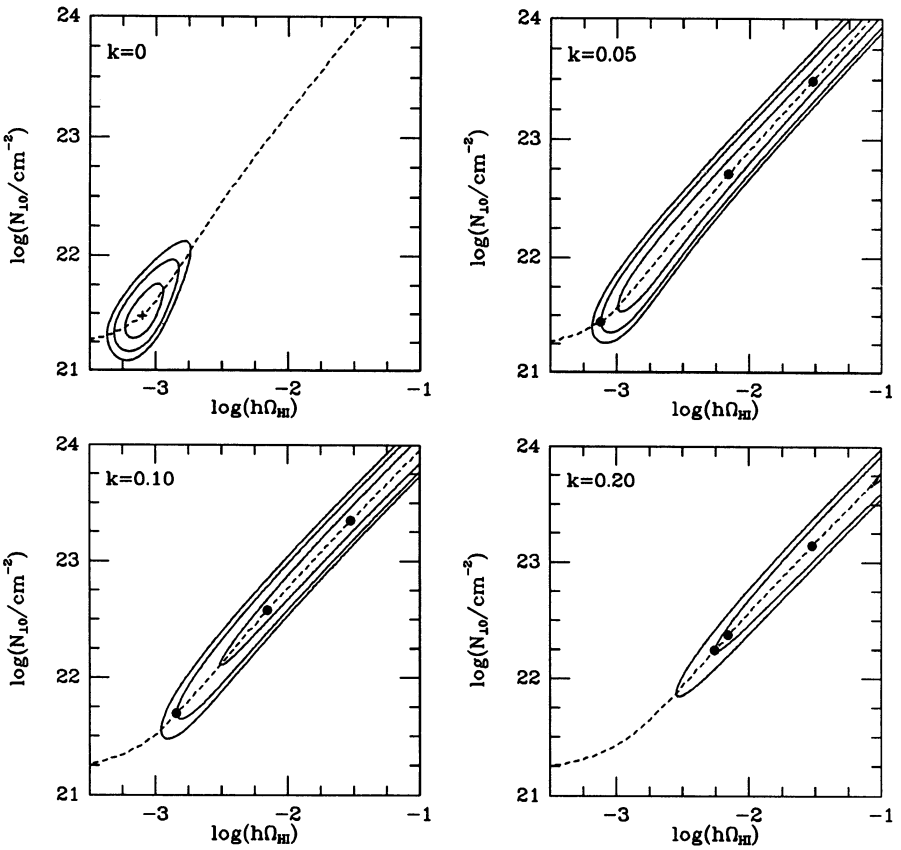


FIG. 3.—Results of the likelihood-ratio tests for $q_0 = 0$. The solid curves show the 1, 2, and 3 $\sigma$ confidence contours for the parameters $h\Omega_{\rm H\,I}$ and $N_{\perp 0}$, and the dashed curves show the maxima of $L(h\Omega_{\rm H\,I}, N_{\perp 0})$ with respect to $N_{\perp 0}$ at constant $h\Omega_{\rm H\,I}$. The cross indicates the best-fit solution without dust ($k = 0$), and the dots indicate the minimum-, intermediate-, and maximum-$\Omega_{\rm H\,I}$ solutions with LMC-type dust and $k = 0.05$, 0.10, and 0.20.

and, in particular, the absence of a cutoff at high H I column densities. Thus, from the data now available, we can only set lower limits on $h\Omega_{\rm H\,I}$ and $N_{\perp 0}$. We refer to the model distributions with the smallest values of $h\Omega_{\rm H\,I}$ on the 2 $\sigma$ confidence contours as "minimum-$\Omega_{\rm H\,I}$" solutions. These are indicated by dots in Figure 3 for $q_0 = 0$ and listed in Table 1 for $q_0 = 0$ and 0.5.

To set upper limits on $h\Omega_{\rm H\,I}$, we must appeal to other astrophysical constraints. Clearly, the comoving density of neutral hydrogen and the associated helium in the damped Ly$\alpha$ systems cannot exceed the comoving density of baryons in all forms, which implies $\Omega_{\rm H\,I} \leq 0.76\Omega_{\rm bar}$. The standard model of big bang nucleosynthesis and the observed abundances of the light elements require $h^2\Omega_{\rm bar} \lesssim 1.6 \times 10^{-2}$ (Olive et al. 1990) and hence $h\Omega_{\rm H\,I} \lesssim 3 \times 10^{-2}$ for $h \gtrsim 0.4$. We refer to the model distributions that maximize $L(h\Omega_{\rm H\,I}, N_{\perp 0})$ at $h\Omega_{\rm H\,I} = 3 \times 10^{-2}$ as "maximum-$\Omega_{\rm H\,I}$" solutions. Since the damped Ly$\alpha$ systems are unlikely to contain all the baryons in the universe at $2 \lesssim z \lesssim 3$, we also present "intermediate-$\Omega_{\rm H\,I}$" solutions, defined by the maxima of $L(h\Omega_{\rm H\,I}, N_{\perp 0})$ at $h\Omega_{\rm H\,I} = 7 \times 10^{-3}$. These might be appropriate if the damped Ly$\alpha$ systems contain roughly as much neutral hydrogen as present-day galaxies contain luminous matter.[1] The maximum- and intermediate-$\Omega_{\rm H\,I}$ solutions are indicated by dots in Figure 3

[1] For a mean luminosity density of $2 \times 10^8 h\ L_\odot\ {\rm Mpc}^{-3}$, the mean mass density corresponds to $h\Omega_{\rm lum} \approx 7 \times 10^{-4} \langle M_{\rm lum}/L_B \rangle$, where $\langle M_{\rm lum}/L_B \rangle \approx 10$ is the luminosity-weighted mean mass-to-light ratio in solar units.

TABLE 1

PARAMETERS OF THE MODEL DISTRIBUTIONS

| | | $q_0 = 0.0$ | | $q_0 = 0.5$ | |
|---|---|---|---|---|---|
| $k$ | SOLUTION | $h\Omega_{\rm H\,I}/10^{-3}$ | $N_{\perp 0}/10^{21}$ cm$^{-2}$ | $h\Omega_{\rm H\,I}/10^{-3}$ | $N_{\perp 0}/10^{21}$ cm$^{-2}$ |
| 0.05..... | min-$\Omega_{\rm H\,I}$ | 0.8 | 2.8 | 1.4 | 2.8 |
| | int-$\Omega_{\rm H\,I}$ | 7.0 | 52 | 7.0 | 23 |
| | max-$\Omega_{\rm H\,I}$ | 30 | 310 | 30 | 150 |
| 0.10..... | min-$\Omega_{\rm H\,I}$ | 1.4 | 4.9 | 2.6 | 4.8 |
| | int-$\Omega_{\rm H\,I}$ | 7.0 | 38 | 7.0 | 17 |
| | max-$\Omega_{\rm H\,I}$ | 30 | 220 | 30 | 100 |
| 0.20..... | min-$\Omega_{\rm H\,I}$ | 5.5 | 18 | 10 | 17 |
| | int-$\Omega_{\rm H\,I}$ | 7.0 | 24 | ... | ... |
| | max-$\Omega_{\rm H\,I}$ | 30 | 140 | 30 | 67 |

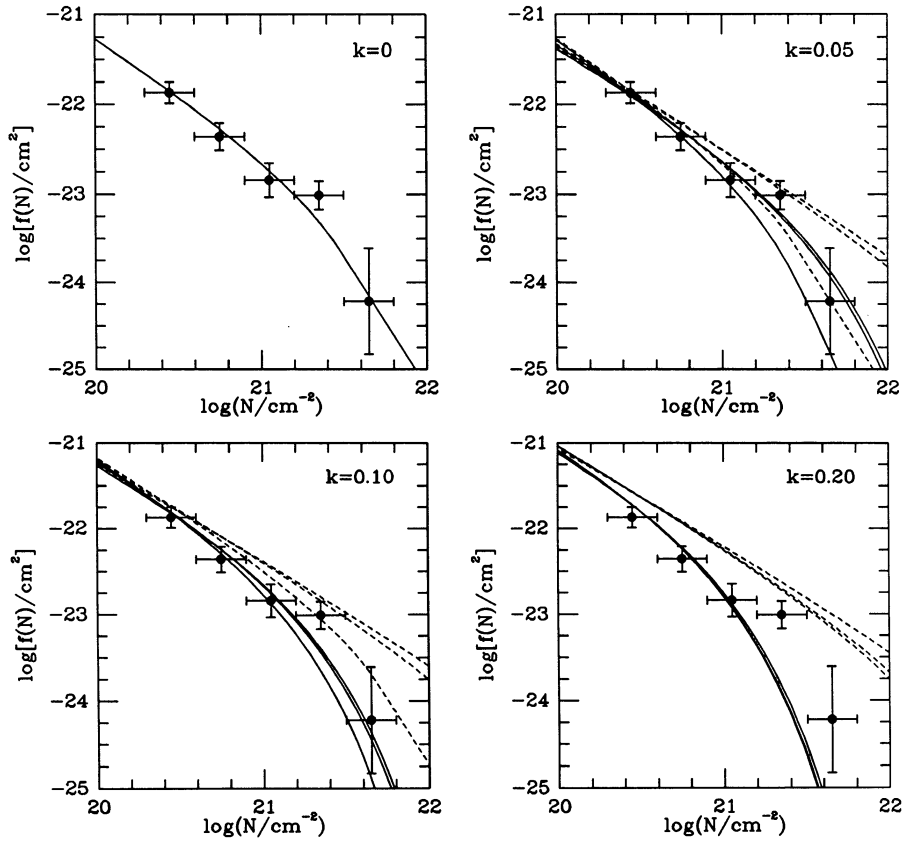


FIG. 4.—Comparison of the model and empirical distributions of H I column densities in damped Lyα systems for $q_0 = 0$. The solid curves show $f_o$, and the dashed curves show $f_t$ for the best-fit solution without dust ($k = 0$) and the minimum-, intermediate-, and maximum-$\Omega_{\rm H\,I}$ solutions with LMC-type dust and $k = 0.05$, 0.10, and 0.20.

for $q_0 = 0$ and listed in Table 1 for $q_0 = 0$ and 0.5. We disregard the intermediate-$\Omega_{\rm H\,I}$ solution with $k = 0.20$ and $q_0 = 0.5$ because it lies outside the 2 $\sigma$ contour.

Figure 4 shows the model distributions $f_t$ (dashed curves) and $f_o$ (solid curves) discussed above together with the empirical distribution of H I column densities in the damped Lyα systems. This illustrates our conclusion from the likelihood-ratio test that acceptable fits can be obtained over wide ranges in the parameters $h\Omega_{\rm H\,I}$ and $N_{\perp 0}$. However, as the dust-to-gas ratio increases, the model distributions $f_t$ and $f_o$ diverge at smaller H I column densities and $f_o$ becomes steeper than the empirical distribution. A $\chi^2$ test indicates that the models with $k = 0$, 0.05, and 0.10 are acceptable, whereas the models with $k = 0.20$ are not. This behavior is largely independent of the assumed H I profiles of the damped Lyα systems, as the following argument shows. According to equation (21), $f_t$ and $f_o$ diverge exponentially for

$$\beta\left(\frac{kN}{10^{21}\ \mathrm{cm}^{-2}}\right)\xi\left(\frac{\lambda_B}{1+z}\right) \approx \left(\frac{k}{0.15}\right)\left(\frac{N}{10^{21}\ \mathrm{cm}^{-2}}\right) \gtrsim 1 . \quad (28)$$

Thus, for $k \gtrsim 0.15$, we expect poor fits over much of the observed range in $N$. This is another reason, in addition to the absence of strong extinction at 2200 Å, for rejecting the large dust-to-gas ratio derived from the observed reddening with the Galactic extinction curve. While $k = 0.20$ is formally excluded, we adopt it as a conservative upper limit in the remainder of this paper. As shown in the Appendix, a dispersion in the dust-to-gas ratio would have little effect on our comparisons between the model and empirical distributions of H I column densities.

The comoving density of dust in the damped Lyα systems can be estimated from the dust-to-gas ratio and the comoving density of H I. The relevant expression is $\Omega_{\rm dust} = kl\Omega_{\rm H\,I}$, where $l$ depends on the physical and optical properties of the grains. Pei (1992) finds $0.013 \lesssim l \lesssim 0.023$ for mixtures of graphite and silicates that reproduce the observed extinction curves in the Milky Way, LMC, and SMC. Thus, we have $10^{-6} \lesssim h\Omega_{\rm dust} \lesssim 10^{-4}$, with most of the range attributable to the weak constraints on $\Omega_{\rm H\,I}$. If the dust were heated to a temperature $T_{\rm dust}$, it would make the following contribution to the mean intensity of background radiation at an observed frequency $\nu$:

$$\Delta J_\nu = \frac{3cH_0}{8\pi G}\int_2^3 dz\, \frac{\Omega_{\rm dust}\kappa_{\nu'} B_{\nu'}(T_{\rm dust})}{(1+z)^2(1+2q_0 z)^{1/2}} . \quad (29)$$

Here, $\kappa_{\nu'}$ and $B_{\nu'}$ are the opacity and Planck function at the emitted frequency $\nu' = \nu(1+z)$, and the integration is conservatively restricted to $2 \le z \le 3$. Current limits from the DIRBE and FIRAS experiments on the *Cosmic Background Explorer* (*COBE*) are $\Delta J_\nu \lesssim 4 \times 10^{-17}$ ergs s$^{-1}$ cm$^{-2}$ Hz$^{-1}$ sr$^{-1}$ at wavelengths from 50 $\mu$m to 1 cm (Mather et al. 1990; Hauser et al. 1991). Equation (29) then implies $T_{\rm dust} \lesssim 60$, 40, and 25 K, respectively, for $h\Omega_{\rm dust} = 10^{-6}$, $10^{-5}$, and $10^{-4}$. Evidently, the dust in the damped Lyα systems cannot be much hotter than the dust in the Milky Way (which has $T_{\rm dust} \approx 20$ K;

Wright et al. 1991). The constraints this imposes on the star formation rates in the damped Lyα systems are discussed in a separate paper (Charlot & Fall 1993).

## 4. OBSCURATION OF QUASARS

We now return to the obscuration of quasars. We continue to model the damped Lyα systems as randomly oriented exponential disks with the constraints on the mean comoving density of H I and the central H I column density derived in the previous section. Here, however, it proves convenient to reexpress these parameters in terms of the corresponding optical depths

$$\tau_* \equiv 104kh\Omega_{\rm H\,I} \quad \text{and} \quad \tau_{\perp 0} \equiv kN_{\perp 0}/10^{21}\ \text{cm}^{-2}\ . \quad (30)$$

The mean optical depth along random lines of sight and the ratio of the true and observed luminosity functions of quasars, from equations (18), (20), (21), and (26), then take the forms

$$\bar{\tau}_t(z) = \int_0^z dz' \frac{\tau_*(z')(1+z')}{(1+2q_0 z')^{1/2}} \xi\left(\frac{\lambda_B}{1+z'}\right), \quad (31)$$

$$\frac{\psi_t(z)}{\psi_o(z)} = \exp\left\{\int_0^z dz' \frac{\tau_*(z')(1+z')}{\tau_{\perp 0}(z')(1+2q_0 z')^{1/2}} \times F\left[\beta\tau_{\perp 0}(z')\xi\left(\frac{\lambda_B}{1+z'}\right)\right]\right\}, \quad (32)$$

with

$$F(x) \equiv \frac{1}{4}\int_0^1 ds s^{-1}(1-2\ln s)[1-\exp(-sx)] + \frac{1}{4}\int_1^\infty ds s^{-3}[1-\exp(-sx)]\ . \quad (33)$$

As expected, $\bar{\tau}_t$ depends only on $\tau_*$, whereas $\psi_t/\psi_o$ depends on both $\tau_*$ and $\tau_{\perp 0}$. The function $F$ defined in equation (33) is plotted in Figure 5.

Since $\bar{\tau}_t(z)$ and $\psi_t(z)/\psi_o(z)$ depend on the absorbers at all redshifts between 0 and $z$, we must consider the possibility that the parameters $\tau_*$ and $\tau_{\perp 0}$ also vary with redshift. Such evolution could be the result of chemical enrichment, consumption of gas by star formation, galactic inflows or outflows, mergers between galaxies, and so forth. Rather than attempt to model these complicated processes, we interpolate between the parameters in the damped Lyα systems and those in present-day galaxies using the simple formulae

$$\tau_*(z) = \tau_*(0)(1+z)^\delta \quad \text{and} \quad \tau_{\perp 0}(z) = \tau_{\perp 0}(0)(1+z)^\epsilon\ . \quad (34)$$

The mean redshift of the damped Lyα systems used in the determination of the dust-to-gas ratio and the distribution of H I column densities is $\bar{z} = 2.4$. Thus, we fix the exponents $\delta$ and $\epsilon$ in equation (34) by $\tau_*(0)$ and $\tau_{\perp 0}(0)$ and the conditions $\tau_*(2.4) = \tau_*(0)(3.4)^\delta$ and $\tau_{\perp 0}(2.4) = \tau_{\perp 0}(0)(3.4)^\epsilon$. Fortunately, our results depend only weakly on $\tau_*(0)$ and $\tau_{\perp 0}(0)$. The reason for this is that the extinction curve declines with wavelength, roughly as $\xi(\lambda) \propto \lambda^{-1}$, which tends to give more weight to the parameters at high redshifts in equations (31) and (32).

We estimate $\tau_*(0)$ as follows. The evidence from a variety of searches for 21 cm emission is that most of the H I in the local universe is associated with optically visible galaxies (Briggs 1990, and references therein). Thus, to a good approximation, the present mean density of H I can be computed from

$$\Omega_{\rm H\,I}(0) = 3.6\times 10^{-12}h^{-2}(\mathscr{L}_B/L_\odot\ \text{Mpc}^{-3})\langle M_{\rm H\,I}/L_B\rangle\ , \quad (35)$$

where $\mathscr{L}_B$ is mean luminosity density in the $B$ band and $\langle M_{\rm H\,I}/L_B\rangle$ is the luminosity-weighted mean H I mass-to-light ratio in solar units. We adopt $\mathscr{L}_B \approx 2\times 10^8 h\ L_\odot\ \text{Mpc}^{-3}$ (Efstathiou, Ellis, & Peterson 1988). Huchtmeier & Richter (1988) list the H I masses and $B$ luminosities of all known late-type galaxies (Sa to Im) with distances less than $5h^{-1}$ Mpc. Dividing the sum of the H I masses by the sum of the $B$ luminosities, we obtain $\langle M_{\rm H\,I}/L_B\rangle = 0.37$. This should be reduced by about 20% to account for the absence of early-type galaxies (E and S0) in the Huchtmeier-Richter sample. We then have $\Omega_{\rm H\,I}(0) \approx 2\times 10^{-4}h^{-1}$ and hence $\tau_*(0) \approx 0.02\bar{k}(0)$, where $\bar{k}(0)$ is the H I–weighted mean dust-to-gas ratio in galaxies at the present epoch. Unfortunately, there is very little direct information about $\bar{k}(0)$, but judging from the abundances of heavy elements in nearby spiral galaxies, it probably lies within a factor of 3 of the Galactic dust-to-gas ratio $k \approx 0.8$. We therefore consider the range $0.005 \lesssim \tau_*(0) \lesssim 0.05$.

The parameter $\tau_{\perp 0}(0)$ is also hard to estimate. Traditionally, the face-on optical depths of spiral galaxies have been inferred from the dependence of the surface brightness $\mu$ on the viewing angle $i$ (Holmberg 1975). This method, however, can give ambiguous results; $\mu$ would vary with $i$ in the same way for a completely transparent disk as it would for a disk with an opaque layer of dust sandwiched between two layers of stars (Disney, Davies, & Phillipps 1989). In a recent study, Valentijn (1990) found little or no correlation between the central surface brightnesses and the projected axial ratios in a large sample of late-type galaxies. He argues from this that the central regions of the galaxies are optically thick, with $\tau_{\perp 0}(0) \approx 1.3$. Another way to estimate $\tau_{\perp 0}(0)$ is from the observed distributions of gas and an assumed dust-to-gas ratio. The peaks in the face-on H I column densities of most spiral galaxies lie in the range $3\times 10^{20} \lesssim N_{\perp\rm max} \lesssim 12\times 10^{20}\ \text{cm}^{-2}$ (Wevers, van der Kruit, & Allen 1986; Warmels 1988a, b). Many of the H I profiles have central "holes," with extrapolated central H I column densities several times higher than $N_{\perp\rm max}$, and many of the holes are filled in by molecular hydrogen (Young & Scoville 1991). These observations, combined with the Galactic dust-to-gas ratio, suggest that central face-on optical depths of a few

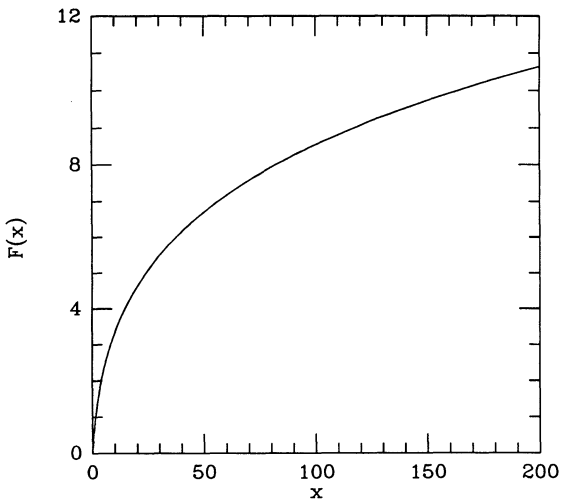


FIG. 5.—Nondimensional function defined in eq. (33) as an intermediate step in the calculation of $\psi_t/\psi_o$.

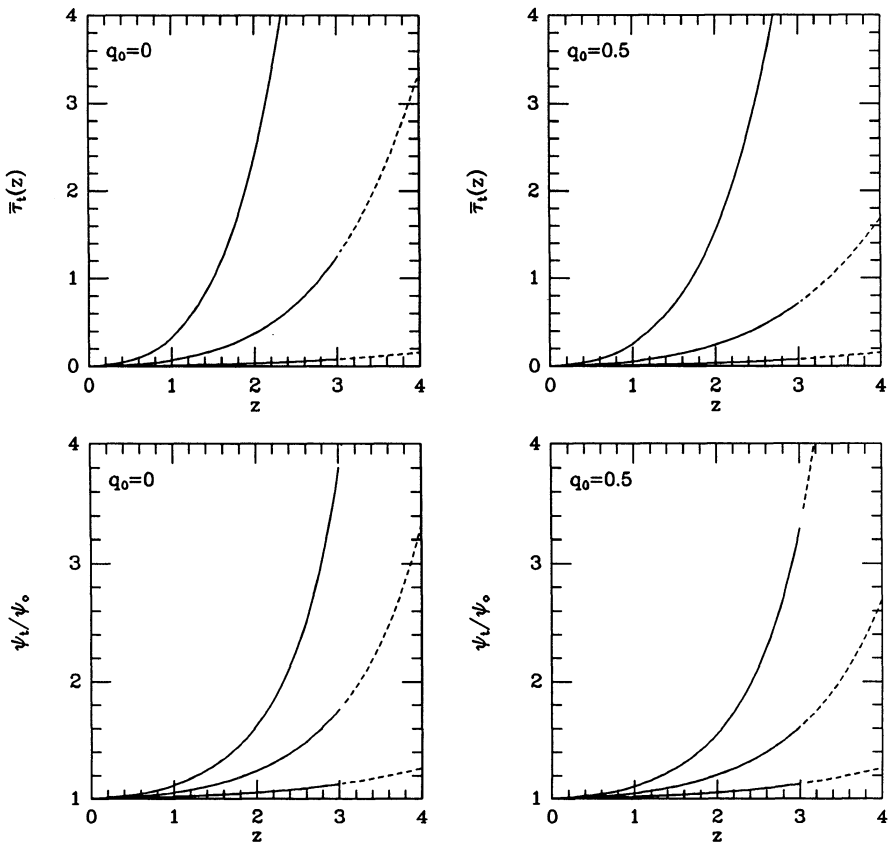


FIG. 6.—Dependence of the mean optical depth along random lines of sight and the ratio of the true and observed luminosity functions of quasars on redshift for $q_0 = 0$ and 0.5. The three curves correspond to models A, B, and C, with the parameters listed in Table 2. The dashed parts of the curves are extrapolations.

may be typical at the present epoch. In the following, we consider the range $0.5 \leq \tau_{\perp 0}(0) \leq 5$.

We now focus on the three models specified in Table 2. Model A corresponds to the minimum-$\Omega_{\rm H\,I}$ solution with $k = 0.05$ and the smallest values of $\tau_*(0)$ and $\tau_{\perp 0}(0)$; model B corresponds to the intermediate-$\Omega_{\rm H\,I}$ solution with $k = 0.10$ and intermediate values of $\tau_*(0)$ and $\tau_{\perp 0}(0)$; and model C corresponds to the maximum-$\Omega_{\rm H\,I}$ solution with $k = 0.20$ and the largest values of $\tau_*(0)$ and $\tau_{\perp 0}(0)$. For the reasons given above, models A and C should provide lower and upper limits to the obscuration, while model B should provide the most realistic estimates. The mean optical depth and the ratio of the true and observed luminosity functions of quasars are plotted against redshift in Figure 6 for each of the three models and for $q_0 = 0$ and 0.5. Table 3 lists the values of $\bar{\tau}_t$ and $\psi_t/\psi_o$ at $z = 2$, 3, and 4, those at $z = 4$ being extrapolations. For $z = 3$, we find $0.08 \leq \bar{\tau}_t \leq 10.3$ and $1.1 \leq \psi_t/\psi_o \leq 3.8$. The wide range in $\bar{\tau}_t$ reflects the weak constraints on $\Omega_{\rm H\,I}$ discussed in the previous section, while the relatively narrow range in $\psi_t/\psi_o$ is a consequence of the strong correlation between $\Omega_{\rm H\,I}$ and $N_{\perp 0}$ depicted in Figure 3. As shown in the Appendix, a dispersion in the dust-to-gas ratio can have a large effect on the mean optical depth but remarkably little effect on the ratio of the true and observed luminosity functions of quasars. This is fortunate because $\psi_t/\psi_o$ provides a more direct measure of obscuration than $\bar{\tau}_t$. Our most realistic estimate, from model B, is $\psi_t/\psi_o \approx 1.7$ at $z = 3$.

TABLE 2

PARAMETERS OF THE OBSCURATION

| | $q_0 = 0.0$ | | $q_0 = 0.5$ | | | |
|---|---|---|---|---|---|---|
| MODEL | $\tau_*(2.4)$ | $\tau_{\perp 0}(2.4)$ | $\tau_*(2.4)$ | $\tau_{\perp 0}(2.4)$ | $\tau_*(0)$ | $\tau_{\perp 0}(0)$ |
| A..... | 0.004 | 0.14 | 0.007 | 0.14 | 0.005 | 0.5 |
| B..... | 0.073 | 3.76 | 0.073 | 1.72 | 0.016 | 1.6 |
| C..... | 0.624 | 27.7 | 0.624 | 13.4 | 0.050 | 5.0 |

TABLE 3

OBSCURATION OF QUASARS AT $z = 2$, 3, AND 4

| | $q_0 = 0.0$ | | | $q_0 = 0.5$ | | | $q_0 = 0.0$ | | | $q_0 = 0.5$ | | |
|---|---|---|---|---|---|---|---|---|---|---|---|---|
| MODEL | $\bar{\tau}_t(2)$ | $\bar{\tau}_t(3)$ | $\bar{\tau}_t(4)$ | $\bar{\tau}_t(2)$ | $\bar{\tau}_t(3)$ | $\bar{\tau}_t(4)$ | $\psi_t(2)/\psi_o(2)$ | $\psi_t(3)/\psi_o(3)$ | $\psi_t(4)/\psi_o(4)$ | $\psi_t(2)/\psi_o(2)$ | $\psi_t(3)/\psi_o(3)$ | $\psi_t(4)/\psi_o(4)$ |
| A..... | 0.04 | 0.08 | 0.16 | 0.04 | 0.08 | 0.16 | 1.05 | 1.13 | 1.26 | 1.06 | 1.13 | 1.27 |
| B..... | 0.37 | 1.26 | 3.36 | 0.24 | 0.71 | 1.70 | 1.24 | 1.77 | 3.33 | 1.21 | 1.61 | 2.71 |
| C..... | 2.40 | 10.3 | 33.3 | 1.54 | 5.72 | 16.5 | 1.63 | 3.80 | 18.0 | 1.56 | 3.30 | 13.0 |

Our results are most directly comparable with those of Heisler & Ostriker (1988) and Wright (1990). We have followed them in assuming that the absorbers can be represented by randomly oriented exponential disks, although there are differences in the methods of computation, the luminosity function of quasars, and the extinction curve of the dust. The most important difference, however, lies in the values of the parameters that control the obscuration. Heisler & Ostriker adopted $\tau_* = 0.2$ and $\tau_{\perp 0} = 0.5$ and found $\bar{\tau}_t \approx 2$ and $\psi_t/\psi_o \approx 12$ at $z = 3$ (see their Fig. 5). Wright tried several combinations of parameters, favoring $(\tau_*, \tau_{\perp 0}) = (0.07, 0.5)$ and $(0.16, 2.0)$, and found $\psi_t/\psi_o \approx 2.7$ and 4.0 at $z = 3$ (see his Fig. 6). In both of these studies, the parameters were assumed to be independent of redshift. The values of $\tau_*$ and $\tau_{\perp 0}$ adopted by Heisler & Ostriker and Wright, when translated into $h\Omega_{\rm H\,I}$ and $N_{\perp 0}$ with $0.05 \leq k \leq 0.20$, lie well outside the 3 $\sigma$ contours in Figure 3. The sense of the discrepancy is that the absorbers in their models cover a larger fraction of the sky than the damped Ly$\alpha$ systems. Wright was guided in part by earlier estimates of the dust-to-gas ratio (from Paper II) and the distribution of H I column densities (from Tytler 1987). His values of $\psi_t/\psi_o$, while within our allowed range, are higher than our most realistic estimate.

Figure 7 shows Hartwick & Schade's (1990) determination of the comoving density of optically selected quasars brighter than $M_B = -26$ as a function of redshift. We have plotted their results separately for the two extreme combinations of the deceleration parameter and spectral index: $(q_0, \alpha) = (0.1, -1.0)$ and $(0.5, -0.5)$. The solid lines in Figure 7 represent our estimates of the true comoving density of bright quasars, i.e., the product of the observed comoving density and the correction factor $\psi_t/\psi_o$, for models A, B, and C. Evidently, the form of the relation depends as much on $q_0$ and $\alpha$ as it does on the parameters of the obscuration. Nevertheless, for each combination of $q_0$ and $\alpha$, the true comoving density has qualitatively the same behavior as the observed comoving density. It increases rapidly in the interval $0 \leq z \lesssim 2$ and then increases or decreases gradually in the interval $2 \lesssim z \lesssim 3$. We therefore conclude that the flattening or turnover in the observed comoving density of bright quasars is not an artifact of obscuration by dust in damped Ly$\alpha$ systems. However, our extrapolations indicate that obscuration might become important at higher redshifts; in extreme cases (e.g. model C), the true and observed comoving densities could differ by more than an order of magnitude at $z = 4$. This possibility should be borne in mind when interpreting the results of the very deep optical surveys now in progress (Irwin, McMahon, & Hazard 1991; Schmidt, Schneider, & Gunn 1991; Warren, Hewett, & Osmer 1991).

A related issue concerns the contribution of quasars to the ultraviolet background radiation at high redshifts (Bechtold et al. 1987; Miralda-Escudé & Ostriker 1990; Madau 1992; Zhou & Phinney 1992). The mean intensity of radiation at a frequency $\nu$ and a redshift $z$ is given by

$$J_\nu(z) = \frac{c}{4\pi H_0}\int_z^\infty dz' \left(\frac{1+z}{1+z'}\right)^3 \frac{\epsilon_t(\nu', z') \exp\left[-\tau_{\rm eff}(\nu, z, z')\right]}{(1+z')^2(1+2q_0 z')^{1/2}}, \quad (36)$$

where $\epsilon_t(\nu', z')$ is the proper emissivity at a frequency $\nu' = \nu(1+z')/(1+z)$ and a redshift $z'$, and $\tau_{\rm eff}(\nu, z, z')$ is the effective optical depth for photoelectric absorption within Ly$\alpha$ forest, Lyman-limit, and damped Ly$\alpha$ systems. (The absorption by dust in damped Ly$\alpha$ systems makes a negligible contribution to $\tau_{\rm eff}$.) For $z \gtrsim 1$, most of the absorption occurs relatively close to the emission, and equation (36) can be approximated by

$$J_\nu(z) \approx \frac{c\epsilon_t(\nu, z)\delta z}{4\pi H_0(1+z)^2(1+2q_0 z)^{1/2}}, \quad (37)$$

with

$$\delta z \equiv \int_z^\infty dz' \exp\left[-\tau_{\rm eff}(\nu, z, z')\right]. \quad (38)$$

Using Madau's (1991) formula for $\tau_{\rm eff}$, we compute $\delta z \approx 0.2$ at the Lyman limit, $\nu = \nu_L$, and $z = 3$.

The true emissivity of quasars is given by an integral over the true luminosity function:

$$\epsilon_t(\nu, z) = 3.3 \times 10^{18}(1+z)^3(\nu/\nu_B)^\alpha \times \int_0^\infty dL \phi_t(L, z)(L/L_{B\odot}) \text{ ergs s}^{-1}\text{ Hz}^{-1}. \quad (39)$$

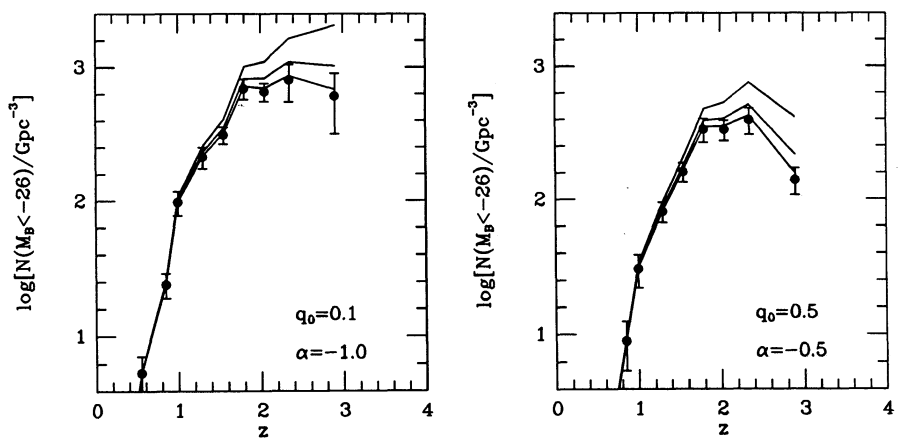


FIG. 7.—Comoving density of quasars brighter than $M_B = -26$ as a function of redshift for $h = 0.5$ and $(q_0, \alpha) = (0.1, -1.0)$ and $(0.5, -0.5)$. The data points and 1 $\sigma$ error bars are from Hartwick & Schade (1990). The solid lines show the true comoving densities corresponding to models A, B, and C, with the parameters listed in Table 2.

We approximate this by $\epsilon_t \approx (\psi_t/\psi_o)\epsilon_o$, where $\epsilon_o$ is the "observed" emissivity of optically selected quasars. A direct sum over the Hartwick & Schade (1990) luminosity function in the interval $2.5 \leq z \leq 3.3$ gives $\epsilon_o(\nu_L, z) \approx 1.7 \times 10^{-47}$ ergs s$^{-1}$ cm$^{-3}$ Hz$^{-1}$ for $(q_0, \alpha) = (0.5, -0.5)$ and $\epsilon_o(\nu_L, z) \approx 1.2 \times 10^{-47}$ ergs s$^{-1}$ cm$^{-3}$ Hz$^{-1}$ for $(q_0, \alpha) = (0.1, -1.0)$. Thus, we find $0.2 \lesssim J_{-21} \lesssim 0.7$ at $z \approx 3$, where $J_{-21}$ is the mean intensity at the Lyman limit in units of $10^{-21}$ ergs s$^{-1}$ cm$^{-2}$ Hz$^{-1}$ sr$^{-1}$. The parameters $q_0$ and $\alpha$ practically cancel out of this calculation, and the quoted range in $J_{-21}$ mainly reflects the range in $\psi_t/\psi_o$ from models A–C. Our estimates of $J_{-21}$ are conservative in the sense that they include only the contribution from quasars brighter than the limiting magnitude $B_l = 22.5$ of the Hartwick & Schade compilation. The contribution from fainter quasars is not known, but plausible extrapolations of the luminosity function indicate that it could increase $J_{-21}$ by a factor of two or so (Koo & Kron 1988). For comparison, the proximity effect in the distribution of Ly$\alpha$ forest systems leads to estimates of the ultraviolet background radiation from all sources in the range $0.3 \lesssim J_{-21} \lesssim 3$ at $z \approx 3$ (Bajtlik, Duncan, & Ostriker 1988; Lu, Wolfe, & Turnshek 1991; Bechtold 1993; Tytler 1993). We conclude that quasars account for at least 10% and possibly all of this radiation.

## 5. DISCUSSION

We have developed a method to compute the obscuration of quasars by dust in damped Ly$\alpha$ systems. The latter are generally believed to be the high-redshift analogs or progenitors of present-day galactic disks. Our calculations are based on the typical dust-to-gas ratio inferred from the reddening of background quasars in our previous studies and the empirical distribution of H I column densities from Lanzetta et al. (1991). We estimate that 10%–70% of the bright quasars at $z = 3$ are obscured by dust in damped Ly$\alpha$ systems and are therefore missing from optical samples. This is not enough obscuration to cause the flattening or turnover in the observed comoving density of bright quasars in the interval $2 \lesssim z \lesssim 3$. Thus, the qualitative behavior of the observed comoving density must reflect the intrinsic evolution of quasars or some bias other than that considered here. This does not mean, however, that the obscuration is entirely negligible. We find that the true comoving density of bright quasars can exceed the observed comoving density by factors up to 4 at $z = 3$. As a consequence, quasars could provide most or even all of the ultraviolet background radiation needed to account for the proximity effect. Moreover, according to our extrapolations, the true comoving density of bright quasars could exceed the observed comoving density by more than an order of magnitude at $z = 4$.

The main uncertainty in our estimates of the obscuration stems from the weak constraints on the number of damped Ly$\alpha$ systems with the highest H I column densities and hence on the comoving density of H I. We find $1 \times 10^{-3} \lesssim h\Omega_{\rm H\,I} \lesssim 3 \times 10^{-2}$, with the upper limit fixed only by the constraints on the comoving density of baryons from big bang nucleosynthesis. The corresponding range in the comoving density of dust is $10^{-6} \lesssim h\Omega_{\rm dust} \lesssim 10^{-4}$. The limits from *COBE* on the far-infrared background radiation imply that the dust in the damped Ly$\alpha$ systems cannot be much hotter than the dust in the Milky Way. If $\Omega_{\rm H\,I}$ is at the upper end of the allowed range, most of the gas in the damped Ly$\alpha$ systems at $2 \lesssim z \lesssim 3$ must have been converted into dark objects (with $M/L_B \gg 1$) by the present epoch. Alternatively, and perhaps more plausibly, the comoving density of gas in the damped Ly$\alpha$ system may be comparable to the comoving density of luminous matter at the present epoch. If so, the intermediate-$\Omega_{\rm H\,I}$ or minimum-$\Omega_{\rm H\,I}$ solutions would be more appropriate than the maximum-$\Omega_{\rm H\,I}$ solutions, and the range of obscuration reduced accordingly. In these cases, the true comoving density of bright quasars exceeds the observed comoving density by less than a factor of 2 at $z = 3$ and less than a factor of 3 at $z = 4$.

Two effects that have been ignored in this paper are obscuration by intergalactic dust and magnification by gravitational lenses. Any dust not associated with the damped Ly$\alpha$ systems would escape detection by our method and cause us to underestimate the true comoving density of bright quasars. Intergalactic dust might be distributed uniformly or in clouds with H I column densities lower than those in the damped Ly$\alpha$ systems. Ostriker et al. (1990) have considered the possible obscuration by dust in C IV absorption-line systems. While some of these may be damped Ly$\alpha$ systems, most of them are probably associated with extended galactic halos or groups of galaxies. None of the searches for intergalactic dust has led to a positive detection, but the constraints on the obscuration are still relatively weak (McKee & Petrosian 1974; Wright 1981; Pei 1991). Magnification by gravitational lenses would have the opposite effect on the relation between the true and observed comoving densities of quasars, especially those brighter than $B \approx 19$ (Fukugita & Turner 1991, and references therein). This issue will be addressed in detail in a separate paper (Pei 1993).

We are grateful to P. Madau, J. P. Ostriker, A. M. Wolfe, and the referee for comments on a draft of this paper.

## APPENDIX

## DISPERSION IN THE DUST-TO-GAS RATIO

Here, we consider how a dispersion in the dust-to-gas ratio in the damped Ly$\alpha$ systems would affect the obscuration of quasars. We define $h_t(N, k, z)dN\,dk\,dX$ and $h_o(N, k, z)dN\,dk\,dX$, respectively, as the mean numbers of absorbers along random and observed lines of sight with H I column densities between $N$ and $N + dN$, dust-to-gas ratios between $k$ and $k + dk$, and absorption distances between $X$ and $X + dX$. The true and observed distributions of H I column densities can be obtained from $h_t$ and $h_o$ by integrating over all $k$ at fixed $N$:

$$f_t(N, z) = \int_0^\infty dk h_t(N, k, z)\,, \tag{A1}$$

$$f_o(N, z) = \int_0^\infty dk h_o(N, k, z)\,. \tag{A2}$$

Furthermore, the true and observed probability densities of the dust-to-gas ratio in absorbers with H I column densities above $N_{\rm min}$ are given by

$$g_t(k, z) = \int_{N_{\rm min}}^{\infty} dN h_t(N, k, z) \Big/ \int_{N_{\rm min}}^{\infty} dN f_t(N, z) , \tag{A3}$$

$$g_o(k, z) = \int_{N_{\rm min}}^{\infty} dN h_o(N, k, z) \Big/ \int_{N_{\rm min}}^{\infty} dN f_o(N, z) . \tag{A4}$$

Since our interest is in the damped Ly$\alpha$ systems, we adopt $N_{\rm min} = 2 \times 10^{20}$ cm$^{-2}$.

The relation between $h_t$ and $h_o$ can be derived most easily in terms of the functions $\rho_t$ and $\rho_o$ introduced in § 2. From the definitions, we have

$$\rho_t(\tau, z)d\tau = (1 + z)(1 + 2q_0 z)^{-1/2} \int_0^{\infty} dk h_t(N, k, z) dN , \tag{A5}$$

$$\rho_o(\tau, z)d\tau = (1 + z)(1 + 2q_0 z)^{-1/2} \int_0^{\infty} dk h_o(N, k, z) dN , \tag{A6}$$

where the integrals must be evaluated at constant optical depth:

$$\tau = \left(\frac{kN}{10^{21}\ {\rm cm}^{-2}}\right) \xi\left(\frac{\lambda_B}{1 + z}\right) . \tag{A7}$$

When the luminosity function of quasars is a power law at the bright end, we have $\rho_t/\rho_o = \exp(\beta t)$ from equation (14) and therefore

$$\frac{h_t(N, k, z)}{h_o(N, k, z)} = \exp\left[\beta\left(\frac{kN}{10^{21}\ {\rm cm}^{-2}}\right)\xi\left(\frac{\lambda_B}{1 + z}\right)\right] . \tag{A8}$$

Equations (A5), (A6), and (A8) are generalizations of equations (15), (16), and (21) to the case of a variable dust-to-gas ratio.

We now assume for simplicity that the H I column densities and dust-to-gas ratios in the damped Ly$\alpha$ systems are statistically independent. This implies

$$h_t(N, k, z) = f_t(N, z) g_t(k, z) . \tag{A9}$$

We then have, from equations (A2), (A4), and (A8),

$$f_o(N, z) = f_t(N, z) \int_0^{\infty} dk g_t(k, z) \exp\left[-\beta a(z) k N\right] , \tag{A10}$$

$$g_o(k, z) = g_t(k, z) \int_{N_{\rm min}}^{\infty} dN f_t(N, z) \exp\left[-\beta a(z) k N\right] \Big/ \int_{N_{\rm min}}^{\infty} dN f_o(N, z) , \tag{A11}$$

with $a(z) \equiv 10^{-21} \xi[\lambda_B/(1 + z)]$ cm$^2$. Evidently, $h_o$ cannot be written as a simple product of $f_o$ and $g_o$. Combining equations (A5), (A9), and (A10) with equations (7) and (11) or (12) gives the mean optical depth along random lines of sight

$$\bar{\tau}_t(z) = 104h \int_0^z dz' \frac{\Omega_{\rm H\,I}(z')(1 + z')}{(1 + 2q_0 z')^{1/2}} \xi\left(\frac{\lambda_B}{1 + z'}\right) \int_0^{\infty} dk g_t(k, z') k , \tag{A12}$$

and the ratio of the true and observed luminosity functions of quasars

$$\frac{\psi_t(z)}{\psi_o(z)} = \exp\left\{\int_0^z dz'(1 + z')(1 + 2q_0 z')^{-1/2} \int_0^{\infty} dN[f_t(N, z') - f_o(N, z')]\right\} . \tag{A13}$$

Equation (A12) is the same as equation (18) except that the mean value of $k$ replaces the constant dust-to-gas ratio; equation (A13) is the same as equation (20) except that $f_t$ and $f_o$ are related by equations (A10) and (A11) instead of equation (21).

To proceed, we must specify the true distributions $f_t$ and $g_t$. We assume, as in the main text, that the absorbers are randomly oriented disks with exponential H I profiles. The true distribution of H I column densities is then given by equation (26). We also assume, somewhat arbitrarily, that the true distribution of dust-to-gas ratios has log-normal form:

$$g_t(k) = \frac{1}{\sqrt{2\pi}\sigma_* k} \exp\left[-\frac{(\ln k - \ln k_*)^2}{2\sigma_*^2}\right] . \tag{A14}$$

This vanishes for $k \to 0$, has a peak at $k = k_* \exp(-\sigma_*^2)$, and declines slowly for $k \to \infty$. The mean and variance of the dust-to-gas ratio are related to the parameters $k_*$ and $\sigma_*$ by

$$\bar{k}_t \equiv \int_0^{\infty} dk g_t(k) k = k_* \exp(\sigma_*^2/2) , \tag{A15}$$

$$\sigma_t^2 \equiv \int_0^{\infty} dk g_t(k)(k - \bar{k}_t)^2 = k_*^2 \exp(\sigma_*^2)\left[\exp(\sigma_*^2) - 1\right] . \tag{A16}$$

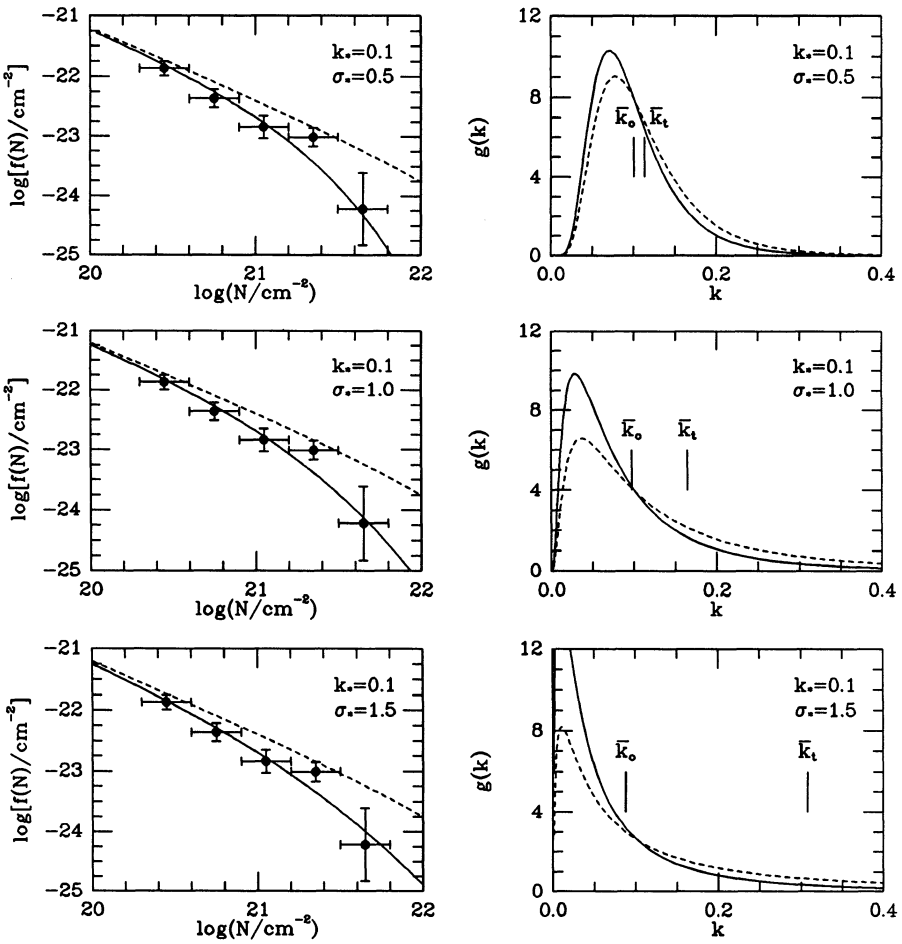


FIG. 8.—Model distributions of H I column densities and dust-to-gas ratios in damped Lyα systems for $q_0 = 0$. The solid curves show $f_o$ and $g_o$, and the dashed curves show $f_t$ and $g_t$ for the intermediate-$\Omega_{\rm H\,I}$ solution with $k_* = 0.1$ and $\sigma_* = 0.5$, 1.0, and 1.5. The data points in the left-hand panels represent the empirical distribution of H I column densities, while the vertical bars in the right-hand panels indicate the means of the true and observed model distributions of dust-to-gas ratios.

As an indication of what one might expect in the damped Lyα systems, we note that galaxies at the present epoch have $\sigma_* \approx \sigma_t/\bar{k}_t \approx 1$ (Pei 1992).

We have computed the observed distributions $f_o$ and $g_o$ from equations (A10) and (A11) with various combinations of the parameters that enter the true distributions $f_t$ and $g_t$. Ideally, we would redetermine $h\Omega_{\rm H\,I}$ and $N_{\perp 0}$ from the likelihood-ratio test for each combination of $k_*$ and $\sigma_*$. In practice, however, this proved unnecessary, and $h\Omega_{\rm H\,I}$ and $N_{\perp 0}$ were fixed at the values derived with a constant dust-to-gas ratio. The left-hand panels of Figure 8 show $f_t$ (dashed curves) and $f_o$ (solid curves) for the intermediate-$\Omega_{\rm H\,I}$ solution with $k_* = 0.1$ and $\sigma_* = 0.5$, 1.0, and 1.5 (corresponding to $\sigma_t/\bar{k}_t = 0.53$, 1.31, and 2.91). In all three cases, $f_o$ provides an acceptable fit to the empirical distribution of H I column densities. As in the case of a constant dust-to-gas ratio, the fraction of missing damped Lyα systems rises with increasing H I column density. The right-hand panels of Figure 8 show $g_t$ (dashed curves) and $g_o$ (solid curves) for the same sets of parameters as the left-hand panels. Both the true and observed distributions of dust-to-gas ratios develop long tails as $\sigma_*$ increases. However, $g_t$ lies above $g_o$ for $k \gtrsim 0.1$, indicating that missing damped Lyα systems tend to be those with the highest dust-to-gas ratios. We find that, although the true mean $\bar{k}_t$ increases rapidly with $\sigma_*$, the observed mean $\bar{k}_o$ remains remarkably close to $k_*$. This suggests that the model distributions with $k_* \approx 0.1$ and $\sigma_* \lesssim 1.5$ are compatible with the observed reddening.

We have computed the mean optical depth along random lines of sight and the ratio of the true and observed luminosity functions of quasars from equations (A12) and (A13) for three models analogous to models A, B, and C. Again, it proves convenient to introduce the parameters $\tau_*$ and $\tau_{\perp 0}$, defined as in equation (30) but with $k$ replaced by the mean dust-to-gas ratio $\bar{k}_t$, and to interpolate between $z = 0$ and $z = 2.4$ using equation (34). We assume that the logarithmic dispersion $\sigma_*$ in the dust-to-gas ratio is independent of redshift and adopt the same values of $\tau_*$ and $\tau_{\perp 0}$ at $z = 0$ as before. However, $\tau_*$ and $\tau_{\perp 0}$ must be increased at $z = 2.4$ to keep $\bar{k}_o$ within the observed range. We therefore retain the previous values of $h\Omega_{\rm H\,I}$ and $N_{\perp 0}$ but set $k_* = 0.05$, 0.10, and 0.20, respectively, for models A, B, and C. We then find $0.05 \leq \bar{k}_o \leq 0.07$ (model A), $0.07 \leq \bar{k}_o \leq 0.10$ (model B), and $0.09 \leq \bar{k}_o \leq 0.20$ (model C) for $\sigma_* \leq 2$. Figure 9 shows $\bar{\tau}_t$ and $\psi_t/\psi_o$ as functions of $\sigma_*$ at $z = 3$ in units of their values with a constant dust-to-gas ratio for each of the three models. Evidently, $\bar{\tau}_t$ is very sensitive to the dispersion in the dust-to-gas ratio for $\sigma_* \gtrsim 1$, whereas $\psi_t/\psi_o$ depends only weakly on $\sigma_*$. This can be understood by referring to equations (A12)–(A15) and Figure 8. The mean optical depth is

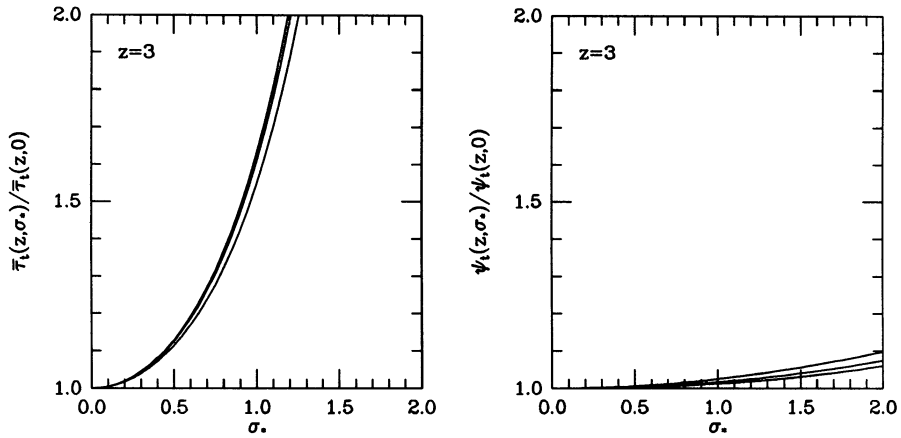


FIG. 9.—Dependence of the obscuration of quasars at $z = 3$ on the logarithmic dispersion of the dust-to-gas ratio in damped Ly$\alpha$ systems for $q_0 = 0$. The mean optical depth along random lines of sight and the ratio of the true and observed luminosity functions of quasars are normalized to their values with a constant dust-to-gas ratio. The three curves in each panel correspond to models A, B, and C, with parameters specified in the Appendix.

proportional to the mean dust-to-gas ratio, which increases rapidly with $\sigma_*$. However, the ratio of the true and observed luminosity functions of quasars depends on the difference between the true and observed distributions of H I column densities, which is hardly affected by $\sigma_*$. We conclude that even a relatively large dispersion in the dust-to-gas ratio would have little effect on our estimates of the true comoving density of quasars.

## REFERENCES


Bahcall, J. N., & Peebles, P. J. E. 1969, ApJ, 156, L7
Bajtlik, S., Duncan, R. C., & Ostriker, J. P. 1988, ApJ, 327, 570
Bechtold, J. 1993, ApJ, in press
Bechtold, J., Weymann, R. J., Lin, Z., & Malkan, M. A. 1987, ApJ, 315, 180
Boissé, P., & Bergeron, J. 1988, A&A, 192, 1
Boyle, B. J., Shanks, T., & Peterson, B. A. 1988, MNRAS, 235, 935
Briggs, F. H. 1990, AJ, 100, 999
Chaffee, F. H., Black, J. H., & Foltz, C. B. 1988, ApJ, 335, 584
Charlot, S., & Fall, S. M. 1993, in preparation
Disney, M., Davies, J., & Phillipps, S. 1989, MNRAS, 239, 939
Efstathiou, G., Ellis, R. S., & Peterson, B. A. 1988, MNRAS, 232, 431
Fall, S. M., & Pei, Y. C. 1989, ApJ, 337, 7 (Paper I)
Fall, S. M., Pei, Y. C., & McMahon, R. G. 1989, ApJ, 341, L5 (Paper II)
Fukugita, M., & Turner, E. L. 1991, MNRAS, 253, 99
Hartwick, F. D. A., & Schade, D. 1990, ARA&A, 28, 437
Hauser, M. G., Kelsall, T., Moseley, S. H., Silverberg, R. F., Murdock, T., Toller, G., Spiesman, W., & Weiland, J. 1991, in After the First Three Minutes, ed. S. S. Holt, C. L. Bennett, & V. Trimble (New York: AIP), 161
Heisler, J., & Ostriker, J. P. 1988, ApJ, 332, 543
Holmberg, E. 1975, in Stars and Stellar Systems, Vol. IX, ed. A. Sandage, M. Sandage, & J. Kristian (University of Chicago Press), 123
Huchtmeier, W. K., & Richter, O.-G. 1988, A&A, 203, 237
Irwin, M., McMahon, R. G., & Hazard, C. 1991, in The Space Density of Quasars, ed. D. Crampton (San Francisco: ASP), 117
Koo, D. C., & Kron, R. G. 1988, ApJ, 325, 92
Lanzetta, K. M., Wolfe, A. M., & Turnshek, D. A. 1989, ApJ, 344, 277
Lanzetta, K. M., Wolfe, A. M., Turnshek, D. A., Lu, L. M., McMahon, R. C., & Hazard, C. 1991, ApJS, 77, 1
Lu, L., Wolfe, A. M., & Turnshek, D. A. 1991, ApJ, 367, 19
Madau, P. 1991, ApJ, 376, L33
———. 1992, ApJ, 389, L1
Mather, J. C., et al. 1990, ApJ, 354, L37
McKee, C. F., & Petrosian, V. 1974, ApJ, 189, 17
Meyer, D. M., & Roth, K. C. 1990, ApJ, 363, 57
Meyer, D. M., Welty, D. E., & York, D. G. 1989, ApJ, 343, L37
Miralda-Escudé, J., & Ostriker, J. P. 1990, ApJ, 350, 1
Najita, J., Silk, J., & Wachter, K. 1990, ApJ, 348, 383
Olive, K. A., Schramm, D. N., Steigman, G., & Walker, T. P. 1990, Phys. Lett. B, 236, 454
Ostriker, J. P., & Heisler, J. 1984, ApJ, 278, 1
Ostriker, J. P., Vogeley, M. S., & York, D. G. 1990, ApJ, 364, 405
Pei, Y. C. 1991, Ph.D. thesis, the Johns Hopkins University
———. 1992, ApJ, 395, 130
———. 1993, in preparation
Pei, Y. C., Fall, S. M., & Bechtold, J. 1991, ApJ, 378, 6 (Paper III)
Pettini, M., Boksenberg, A., & Hunstead, R. W. 1990, ApJ, 348, 48
Sargent, W. L. W., Steidel, C. C., & Boksenberg, A. 1989, ApJS, 69, 703
Schmidt, M., Schneider, D. P., & Gunn, J. E. 1991, in The Space Density of Quasars, ed. D. Crampton (San Francisco: ASP), 109
Turnshek, D. A., Wolfe, A. M., Lanzetta, K. M., Briggs, F. H., Cohen, R. D., Foltz, C. B., Smith, H. E., & Wilkes, B. J. 1989, ApJ, 344, 567
Tytler, D. 1987, ApJ, 321, 49
———. 1993, in preparation
Valentijn, E. A. 1990, Nature, 346, 153
Warmels, R. H. 1988a, A&AS, 72, 427
———. 1988b, A&AS, 73, 453
Warren, S. J., Hewett, P. C., & Osmer, P. S. 1991, in The Space Density of Quasars, ed. D. Crampton (San Francisco: ASP), 139
Wevers, B. M. H. R., van der Kruit, P. C., & Allen, R. J. 1986, A&AS, 66, 505
Wolfe, A. M., Turnshek, D. A., Smith, H. E., & Cohen, R. D. 1986, ApJS, 61, 249
Wright, E. L. 1981, ApJ, 250, 1
———. 1986, ApJ, 311, 156
———. 1990, ApJ, 353, 411
Wright, E. L., et al. 1991, ApJ, 381, 200
Young, J. S., & Scoville, N. Z. 1991, ARA&A, 29, 581
Zhou, L., & Phinney, E. S. 1992, preprint